

AD-A236 191



20030214095

2

TECHNICAL REPORT BRL-TR-3236

BRL

HIGH VELOCITY PERFORMANCE OF
A URANIUM ALLOY LONG ROD PENETRATOR

MICHAEL J. KEELE
EDWARD J. RAPACKI, JR.
WILLIAM J. BRUCHEY, JR.

DTIC
ELECTE
JUN 06 1991
S B D

MAY 1991

APPROVED FOR PUBLIC RELEASE; DISTRIBUTION IS UNLIMITED.

U.S. ARMY LABORATORY COMMAND

BALLISTIC RESEARCH LABORATORY
ABERDEEN PROVING GROUND. MARYLAND

91 6 0 19

91-01174



NOTICES

Destroy this report when it is no longer needed. DO NOT return it to the originator.

Additional copies of this report may be obtained from the National Technical Information Service, U.S. Department of Commerce, 5285 Port Royal Road, Springfield, VA 22161.

The findings of this report are not to be construed as an official Department of the Army position, unless so designated by other authorized documents.

The use of trade names or manufacturers' names in this report does not constitute indorsement of any commercial product.

UNCLASSIFIED

REPORT DOCUMENTATION PAGE			Form Approved OMB No. 0704-0188	
Public reporting burden for this collection of information is estimated to average 1 hour per response, including the time for reviewing instructions, searching existing data sources, gathering and maintaining the data needed, and completing and reviewing the collection of information. Send comments regarding this burden estimate or any other aspect of this collection of information, including suggestions for reducing this burden, to Washington Headquarters Services, Directorate for Information Operations and Reports, 1215 Jefferson Davis Highway, Suite 1204, Arlington, VA 22202-4302, and to the Office of Management and Budget, Paperwork Reduction Project (0704-0188), Washington, DC 20503.				
1. AGENCY USE ONLY (Leave blank)	2. REPORT DATE MAY 1991	3. REPORT TYPE AND DATES COVERED Final, Oct 89 - Sep 90		
4. TITLE AND SUBTITLE High Velocity Performance of a Uranium Alloy Long Rod Penetrator			5. FUNDING NUMBERS PR: 1L162618AH80	
6. AUTHOR(S) Michzel J. Keele, Edward J. Rapacki, Jr., William J. Bruchey, Jr.				
7. PERFORMING ORGANIZATION NAME(S) AND ADDRESS(ES) US Army Ballistic Research Laboratory ATTN: SLCBR-TB-A Aberdeen Proving Ground, MD 21005-5066			8. PERFORMING ORGANIZATION REPORT NUMBER	
9. SPONSORING/MONITORING AGENCY NAME(S) AND ADDRESS(ES) US Army Ballistic Research Laboratory ATTN: SLCBR-DD-T Aberdeen Proving Ground, MD 21005-5066			10. SPONSORING/MONITORING AGENCY REPORT NUMBER BRL-TR-3236	
11. SUPPLEMENTARY NOTES Presented at 12th International Ballistics Symposium, October 1990, San Antonio, TX.				
12a. DISTRIBUTION/AVAILABILITY STATEMENT Approved for public release; distribution is unlimited.			12b. DISTRIBUTION CODE	
13. ABSTRACT (Maximum 200 words) Ballistic test data of a uranium alloy long rod penetrator impacting rolled homogeneous armor over the velocity range of 1.7 to 2.4 km/s are presented. The penetration results of the nominally half-scale penetrator of length-to-diameter ratio 20 are compared to those achieved with tungsten alloy penetrators of similar size and aspect ratio. Results indicate that length normalized penetration (P/L) of the two penetrator materials converge as impact velocity exceeds 2.0 km/s.				
14. SUBJECT TERMS kinetic energy projectiles; hypervelocity projectiles; armor; terminal ballistics			15. NUMBER OF PAGES 24	
			16. PRICE CODE	
17. SECURITY CLASSIFICATION OF REPORT UNCLASSIFIED	18. SECURITY CLASSIFICATION OF THIS PAGE UNCLASSIFIED	19. SECURITY CLASSIFICATION OF ABSTRACT UNCLASSIFIED	20. LIMITATION OF ABSTRACT	

TABLE OF CONTENTS

	<u>Page</u>
LIST OF FIGURES	v
LIST OF TABLES	v
ACKNOWLEDGMENTS	vii
1. INTRODUCTION	1
2. MATERIALS AND METHODS	1
2.1 Projectile Description	1
2.2 Double-Travel 120-mm Gun Tube Description	3
2.3 Propellant Description	3
2.4 Target Description	3
3. TEST METHODS	4
3.1 Launch and Flight Evaluation	4
3.2 Target Evaluation	5
4. TEST RESULTS	6
4.1 Launch and Flight Results	6
4.2 Target Impact Conditions and Penetration Results	8
4.3 Penetration Channel Measurements	8
5. DISCUSSION	8
5.1 Critical Impact Yaw	10
5.2 Penetration Channel Characteristics	11
5.3 High Velocity Penetration Performance Comparison of DU and WHA	11
6. CONCLUSIONS	14
7. REFERENCES	17
DISTRIBUTION LIST	19

INTENTIONALLY LEFT BLANK.

LIST OF FIGURES

<u>Figure</u>		<u>Page</u>
1.	Penetrator Details	2
2.	Semi-Infinite RHA Target Design	4
3.	Target Channel Description	6
4.	"Smear" Image of Sabot Separation at 2.35 km/s	7
5.	Penetration Channel Profiles	10
6.	L/D=20 DU and 90% WHA Penetration Data Compared	13
7.	L/D=10 DU and 97% WHA Penetration Data Compared (Farrand 1990)	13
8.	Semi-Infinite RHA Penetration by 90% WHA L/D 9-30 Penetrators (Sorensen et al. 1989)	15

LIST OF TABLES

<u>Table</u>		<u>Page</u>
1.	U-3/4Ti Penetrator Material Properties	3
2.	Slug Test Results	3
3.	Impact Conditions and Penetration Results	8
4.	Penetration Channel Measurements	9



Accession For	
NTIS GRA&I	<input checked="" type="checkbox"/>
DTIC TAB	<input type="checkbox"/>
Unannounced	<input type="checkbox"/>
Justification	
By _____	
Distribution/	
Availability Codes	
Dist	Avail and/or Special
A-1	

INTENTIONALLY LEFT BLANK.

ACKNOWLEDGMENTS

The authors gratefully acknowledge the assistance of the following individuals for their technical efforts: Mr. Richard Kirkendall, Interior Ballistics Division (IBD), for projectile design; Mssrs. Fred Robbins and Joseph Colburn, IBD, for interior ballistic calculations and testing; Mr. Brett Sorensen, Terminal Ballistics Division (TBD), for slug projectile design; Mssrs. Fred Brandon and Richard Pennekamp, Launch and Flight Division (LFD), for exterior ballistic calculations and data reduction; and last but not least, the personnel of Range 14, Range 9, and Range 18 for their careful attention to detail.

INTENTIONALLY LEFT BLANK.

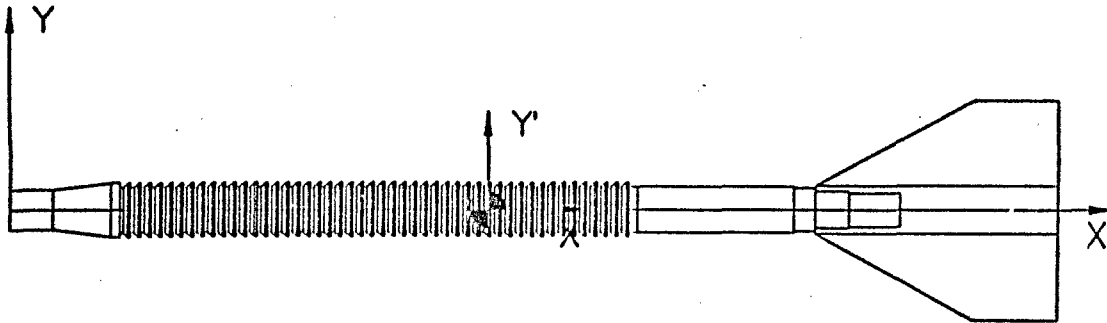
1. INTRODUCTION

The ballistic performance of kinetic energy (KE) penetrators at very high impact velocities (>2.0 km/s) has attracted increased interest from the terminal ballistics community over the past few years. As alternatives to chemical energy propulsion—notably electromagnetic guns—begin to offer high velocity and high energy, appropriate penetrator configurations and materials must be examined. High density, high strength, and other material properties have made tungsten heavy alloys (WHA) and depleted uranium (DU) alloys the materials of choice for KE penetrators. The terminal ballistic capabilities of both alloys have been extensively evaluated and documented at ordnance velocities up to 1.8 km/s, where DU alloys are the superior terminal ballistic performers (Kennedy and Coates 1990a, 1990b; Magness 1986). Tungsten alloys have also been extensively evaluated in the very high velocity regime (Silsby 1984; Sorensen et al. 1989; Hohler and Stulp 1977). However, due to the environmental restrictions associated with testing DU penetrators, the high velocity performance of DU has not been previously investigated. In order to fill this void of DU penetrator data, the unique capabilities of the Ballistic Research Laboratory's (BRL) Range 9 and Range 14 large caliber test facilities were exploited. Specifically, this investigation has centered on the testing of a 120-mm projectile with a nominally half-scale penetrator core of aspect ratio 20, capable of achieving velocities of 2.4 km/s. This paper reports results of semi-infinite penetration tests performed against thick rolled homogeneous armor (RHA) targets impacted at velocities ranging from 1.7 km/s to 2.4 km/s.

2. MATERIALS AND METHODS

An enhanced performance 120-mm launch system in which each component of the system was modified to achieve the highest launch velocity was utilized. Specifically, 1) the in-bore mass of the projectile was made lighter by integrating a nominally half-scale penetrator core with a full-scale sabot, 2) an extended length gun tube was used, and 3) the granular propulsion charge performance was enhanced by heating prior to firing. A detailed description of these modifications follow.

2.1 Projectile Description. The high velocity KE projectile was designed for integration into the 120-mm gun system. The U-3/4Ti alloy penetrator core is nominally half scale and has an aspect ratio of 20 based on the minor diameter (see Figure 1). The thermal-mechanical processing of the penetrator material was in accordance with the specifications for the M833 projectile (see Table 1). The front end is blunt-nosed, and the tail end is fit with a six-blade test fin. The projectile was



In-Flight Mass = 815 g

In-Flight Length = 314 mm

Center of Gravity (from nose) = 145 mm

Penetrator Core Mass = 730 grams

Penetrator Length = 266.7 mm

Penetrator Aspect Ratio = 20

Figure 1. Penetrator Details.

designed without a nose cone to minimize the number of parameters which contribute to the terminal ballistic interaction with the target. The blades of the fin assembly were designed with a large planform area to increase yaw dampening effects, and no cant or bevel angle so that essentially no projectile spin occurred during the launch and flight. A sacrificial coating of RTV* rubber was applied to the aluminum fins for protection against the extreme in-bore temperatures and pressures during launch. This same coating had been effectively used during high velocity KE tests performed by the Penetration Mechanics Branch (PMB) of the Ballistic Research Laboratory (BRL) (Sorensen et al. 1989). The double-ramp sabot was designed according to equations developed by Drysdale (1981). A combination of buttress grooves and screw threads couple the four-piece sabot and penetrator core. The projectile package utilizes a standard 120-mm nylon obturator and standard 120-mm x 570-mm cartridge components. Total in-bore projectile mass was 3.06 kg. This relatively light package weight was the dominant factor for achieving the high launch velocity goal with the 120-mm gun system.

*Dow Chemical Silastic J RTV

Table 1. U-3/4Ti Penetrator Material Properties

Hardness (HRC)	Yield Strength 0.2% Offset (MPa)	Ultimate Tensile Strength (MPa)	Elongation (%)
42	793	1.482	20

2.2 Double-Travel 120-mm Gun Tube Description. A double-travel 120-mm gun tube (serial number 021) was used in place of the standard 120-mm gun tube. It has a total projectile travel length of 9.4 m, and, as the name implies, the double-travel gun tube is nearly twice as long as the standard 120-mm gun tube.

2.3 Propellant Description. Available propellants were screened by computer simulations, and the most promising candidate was found to be a JA-2 formulation, 19 perforation, hexagonal granular configuration. A short series of slug tests were conducted at BRL's Full-Scale Interior Ballistic Range to provide experimental verification of the computational results (Colburn 1991). A monobloc aluminum slug was designed of equal mass and chamber intrusion as that of the KE projectiles. Maximum propellant capacity was 8.78 kg. In order to obtain the highest propellant effectiveness, the loaded cartridges were temperature-conditioned at 63° C for a period of 24 hours prior to firing. This conditioning contributed to an approximate 10% increase in launch velocity. The slug test results are summarized in Table 2.

Table 2. Slug Test Results

CHARGE MASS (kg)	LAUNCH VELOCITY (m/s)	BREECH PRESSURE (MPa)
7.27	2,085	299.2
7.95	2,279	403.3
8.73	2,475	513.6
8.8	2,466	526.1

2.4 Target Description. The semi-infinite RHA target configuration is shown in Figure 2. It was a laminate of four 150-mm-thick RHA (Mil Spec 12560G) plates at 0° obliquity which were bound by

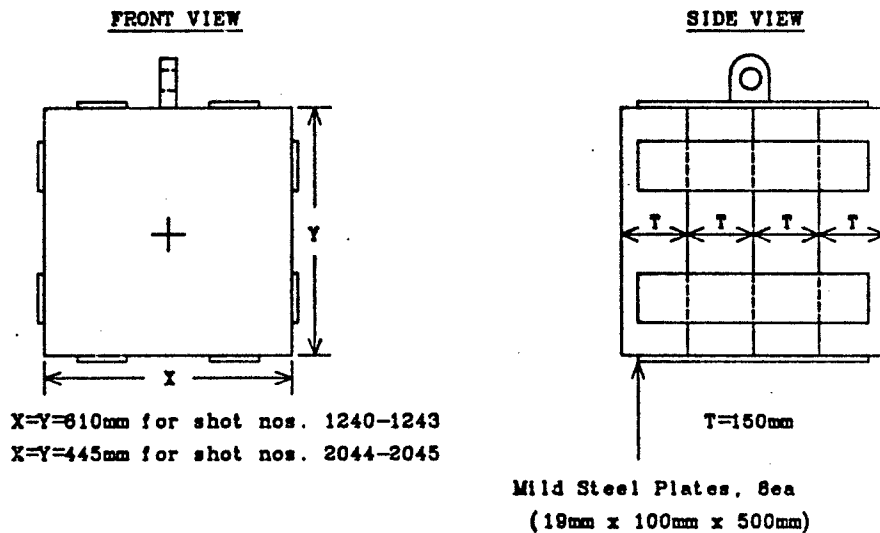


Figure 2. Semi-Infinite RHA Target Design.

mild steel straps welded along the sides of the target. Nominal target hardness was 269 BHN. The targets were sufficiently large so that the presence of the rear and side free surfaces had negligible influence on the anticipated total penetration depths. Because the dispersion and penetration capabilities of the high velocity projectile were initially unknown, the first four targets were built with large presented (610-mm x 610-mm) areas to ensure acceptable impact location on the target. These shots produced acceptable dispersion over the terminal ballistic test range of approximately 75 m; therefore, subsequent RHA targets were designed with a 445-mm x 445-mm presented area.

3. TEST METHODS

3.1 Launch and Flight Evaluation. A total of six KE projectiles were fired against the semi-infinite RHA target configuration. The initial shots were fired with extensive launch and flight diagnostic instrumentation, which included the following: M11 copper crusher chamber pressure gauges, muzzle exit flash radiography, two ballistic synchronized ("smear") cameras, ten yaw card stations (1.5-mm cardboard or 15-lb felt paper), and two sets of orthogonal flash x-ray stations located in front of the target. Once projectile launch and flight were proven successful, less emphasis was placed on launch diagnostics.

The ten yaw card stations were located at 3-m to 6-m intervals uprange of the target. Measurements of the penetrator's flight attitude and orientation at each yaw card station, as well as at the pre-impact x-ray stations which were set up approximately 3-m uprange of the target face, were the primary means of measuring the penetrator's flight characteristics. A sinusoidal function was fit to these yaw data so that a yaw cycle and projected impact yaw estimation could be made. As the yaw cycle estimations accumulated after each shot, more confident predictions of the projectile yaw cycle could be made and were used to readjust the muzzle-to-target distance to yield the most favorable impact conditions.

The penetrator impact velocity and flight orientation just prior to impact were measured directly from the two sets of time-delayed radiographic images in the horizontal and vertical planes. The flight attitude of the penetrator is represented by the total yaw (γ_p) measurement, which is defined as the angular deviation of the penetrator's longitudinal axis from its flight path. The vertical and horizontal components of the total yaw are the pitch (α) and yaw (β), respectively. The orientation angle (ϕ_p) is defined as the angle created by the projection of γ_p onto a plane normal to the flight path with respect to a vertical reference. The orientation angle is measured with positive clockwise rotation as the sign convention. The impact pitch and yaw are typically recorded as projections of uprange yaw measurements. However, the relatively large fin assembly and high impact velocity of this projectile created impact signatures on the front face of the RHA targets similar to those created on the yaw cards. Because this projectile has a short yaw cycle period and its total yaw therefore has a tendency to change rapidly as it travels downrange, the impact yaws were measured directly from the target impact signature. Reasonable correlations between these target impact signature yaw measurements and those predicted by the uprange measurements were obtained.

3.2 Target Evaluation. Several sets of post-impact target measurements were recorded. They included the penetration entrance and exit hole locations and dimensions on each RHA plate comprising the target package. These measurements were used to characterize the hole diameter and the penetration channel orientations associated with the impact. The transverse displacement of the exit hole location relative to the entrance hole was measured and transformed into two angles which describe the penetration channel deviation from the flight path (γ_i) and its orientation (ϕ_i) relative to the vertical (see Figure 3).

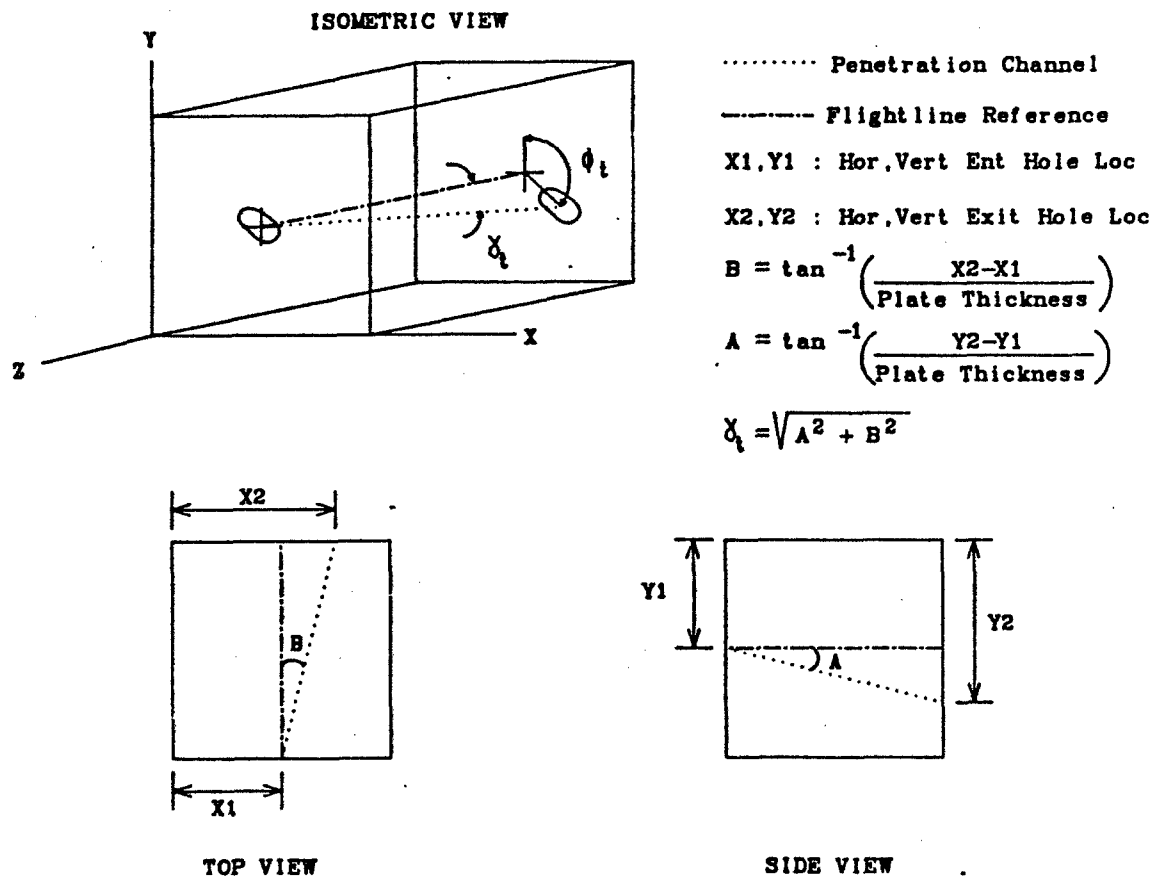


Figure 3. Target Channel Description.

Additional measurements were recorded after the plates were sectioned through the approximate centerline of the penetration channel. These included the maximum depth of penetration and penetration channel diameter measurements taken at small intervals along the penetration channel depth. The maximum depth of penetration was recorded as the sum of the target plate thicknesses less the remaining thickness of RHA not penetrated.

4. TEST RESULTS

4.1 Launch and Flight Results. A large concern during initial testing was the launch integrity of the aluminum sabot and fin assembly during high launch accelerations. "Smear" photographs (Figure 4) were taken at a range of 15 m from the muzzle to show projectile/sabot separation at

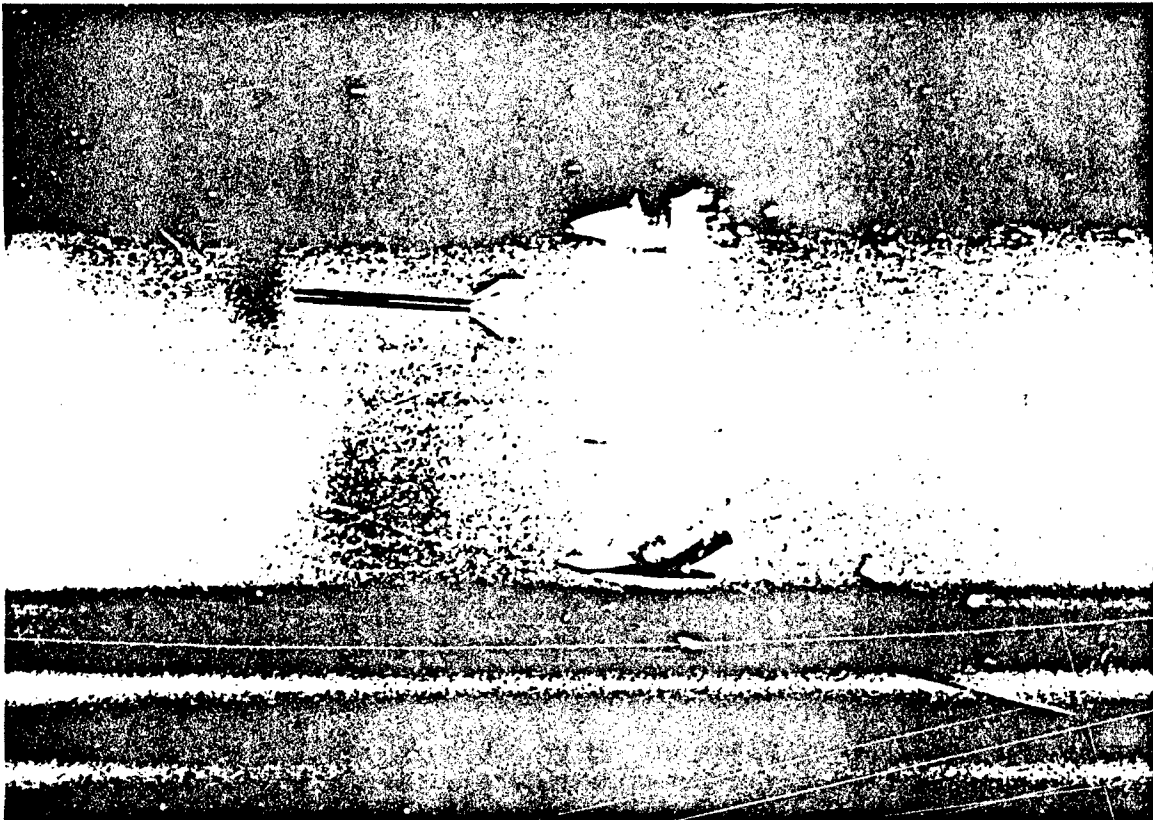


Figure 4. "Smear" Image of Sabot Separation at 2.35 km/s.

a muzzle velocity of approximately 2.35 km/s. The penetrator core appears straight, and the sabot petals have separated cleanly with no indication of binding in the vulnerable saddle area. The fin blades have also survived the initial launch. The pre-impact radiographs revealed that the DU penetrator core maintained its straightness; however, slight flaring of the penetrator nose was evident. It is believed that repetitive high velocity impacts with the yaw cards caused this plastic deformation, regardless of whether the yaw card material was 1.5-mm cardboard or 15-lb felt paper. The diameter of the flare did not exceed the major diameter of the penetrator, and any shortening of the penetrator was minimal. The pre-impact radiographs also revealed a slight loss of leading edge material from the fin blades for impact velocities in excess of 2.0 km/s. The fin damage most likely occurred during the initial combustion stage of the launch when the fin is impacted by propellant grains. Additional ablation most likely occurred due to aerodynamic heating and high velocity impacts with the yaw cards. This may have contributed to inconsistent yaw cycle behavior of the projectile at the higher velocities.

4.2 Target Impact Conditions and Penetration Results. The impact conditions, depth of penetration, and normalized penetration performance (P/L) results are shown in Table 3.

Table 3. Impact Conditions and Penetration Results

SHOT NO.	STRIKING VELOCITY (Vs) (m/s)	PITCH (α) (deg)	YAW (β) (deg)	TOTAL YAW (γ_p) (deg)	ORIENTATION (ϕ_p) (deg)	PENETRATION (P) (mm)	P/L
1240	1,979	↓2.73	→2.14	3.47	141.9	334.0	1.25
1241	2,344	↑2.09	← .76	2.22	340.0	377.5	1.41
1242	2,074	↓ .29	← .33	.44	228.7	347.0	1.30
1243	2,391	↑1.16	← .20	1.18	359.8	388.0	1.45
2044	1,927	↓ .80	←1.99	2.15	248.1	326.0	1.22
2045	1,725	↓ .45	→ .69	.82	123.1	302.0	1.13

4.3 Penetration Channel Measurements. The results of the post-mortem target measurements are listed in Table 4. The penetration channel diameter measurements for the low impact yaw shots (Nos. 1242, 1243, and 2045) are plotted as a function of penetration depth in Figure 5. The channel diameters indicated on the plots correspond to penetration depths of 25, 50, 75, and 90% of the total depth of penetration for each of these shots.

5. DISCUSSION

The main objective of this program was to establish the penetration capabilities of DU at high impact velocities. However, meaningful interpretation and comparisons of depth of penetration results of a KE penetrator test can only be made if the penetrator's impact yaw and yaw rate are zero, or nearly so. In other words, the penetrator's longitudinal axis and velocity vector must be perfectly aligned. This condition is rarely achieved in practice. Significant insight to interpret the results can be obtained from examining the penetration channel hole profiles to determine penetrator/target response to less-than-ideal impact conditions. These aspects will be discussed first, and the remainder of the analysis will focus on the penetration performance capabilities of DU compared to extant WHA data as the impact velocities extend into the high velocity regime.

Table 4. Penetration Channel Measurements

SHOT NO. - PLATE NO.	ENT HOLE DIAMETER (mm)		EXIT HOLE DIAMETER (mm)		CHANNEL ANGLE (γ) (deg)	CHANNEL ORIENT (ϕ) (deg)
	Major	Minor	Major	Minor		
1240-1	31.7	25.4	30.2	28.6	2.45	14
1240-2	30.2	27.0	25.4	25.4	4.86	150
1240-3	15.9	15.9	NA	NA	NM	NM
1241-1	31.7	28.6	34.9	34.9	1.33	153
1241-2	33.3	31.7	30.2	28.6	.60	180
1241-3	28.6	27.0	NA	NA	NM	NM
1242-1	25.4	25.4	30.2	30.2	1.33	27
1242-2	30.2	28.6	NM	NM	1.79	270
1242-3	20.6	19.1	NA	NA	NM	NM
1243-1	30.2	28.6	36.5	36.5	1.33	153
1243-2	33.3	33.3	31.7	27.0	.85	135
1243-3	28.6	25.4	NA	NA	NM	NM
2044-1	28.6	27.0	28.6	28.6	1.19	90
2044-2	28.6	27.0	19.1	19.1	1.89	251
2044-3	15.9	15.9	NA	NA	NM	NM
2045-1	26.2	23.8	28.6	23.8	1.33	296
2045-2	27.0	23.8	NA	NA	NM	NM

Notes: NM = Not Measured
NA = Not Applicable

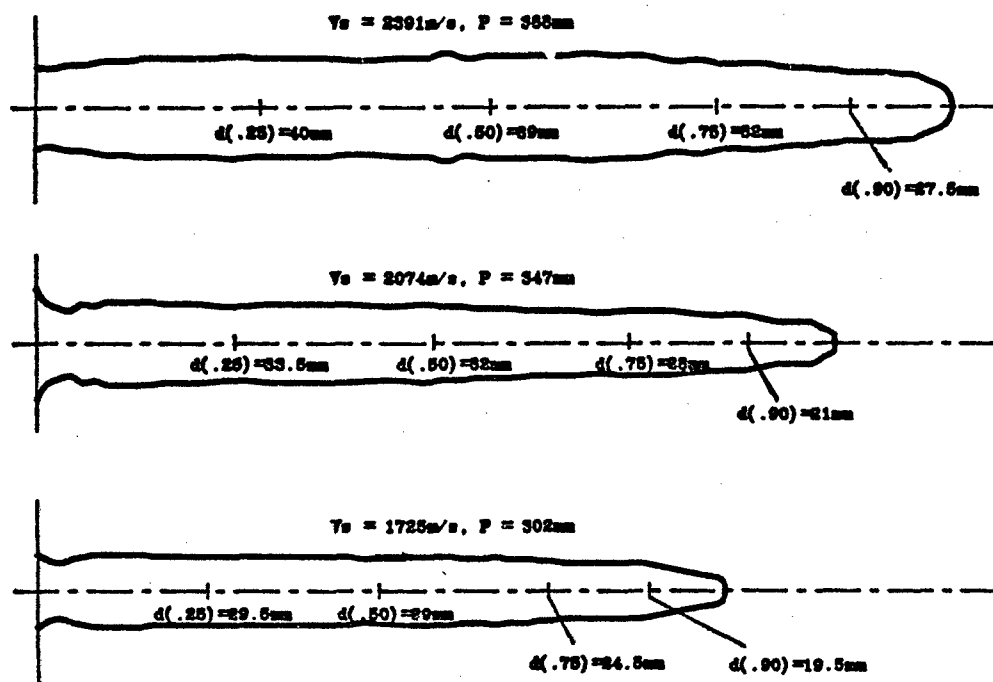


Figure 5. Penetration Channel Profiles.

5.1 Critical Impact Yaw. The model used in this study to determine the maximum impact yaw that minimally affects the depth of penetration was proposed by Silsby, Roszak, and Giglio-Tos (1983). The model is based on a geometric interference argument (i.e., that yaw angle which just allows the entire penetrator to pass through the penetration channel without interference). Utilizing the following equation,

$$\gamma_c = \text{ARCSIN} [(H-D)/2L] \quad (\text{Silsby, Roszak, and Giglio-Tos 1983}), \quad (1)$$

where γ_c = critical impact yaw below which penetration is not affected

H = minor diameter of impact crater

L = initial length of penetrator

D = diameter of penetrator,

the critical impact yaw can be determined. These values range from 1.12° at 1.7 km/s to 1.64° at 2.4 km/s . Larger entrance hole diameters at the higher impact velocities allow a larger impact yaw before collision with the sidewall occurs. No attempt is made here to correct depths of penetration for adverse impact conditions.

5.2 Penetration Channel Characteristics. The impact orientation of a KE long rod penetrator determines the penetration channel orientation and eccentricity. At ordnance velocities, Bjerke et al. (1991) studied the penetration channel orientations in steel targets made by high density tungsten penetrators and observed that the channel is typically a near mirror image of the penetrator impact yaw. The measurements in Table 4 strongly suggest that this holds true for high velocity impacts of a DU penetrator as well. For excessive impact yaw, however, the aft end of the penetrator will bump the side of the penetration channel, causing the penetrator to deviate from its initial impact orientation. The cross-sectional view normal to the penetration channel for these high yaw impact conditions tend to be oblong or "key-holed" shaped, the amount of which depends upon the severity of the impact yaw. Caution must be taken, therefore, when interpreting the diameter measurements. The penetration channel contours detailed in Figure 5 are shown because they had nearly circular cross-sectional profiles due to low total impact yaw.

5.3 High Velocity Penetration Performance Comparison of DU and WHA. The standard method in which long rod, heavy metal KE penetrators of different material and geometry are compared and ranked is the depth of penetration into RHA as a function of impact velocity. Tungsten heavy alloys with 90% to 97% tungsten content and depleted uranium alloys have been extensively studied in a wide variety of long rod geometric configurations. In direct comparison against the semi-infinite RHA target, the U-3/4Ti alloy consistently outperforms the best WHA alloys at ordnance velocities up to 1.8 km/s (Magness 1990a). Both alloy materials, however, follow the same general process of penetration. When a long rod penetrator impacts a steel target at ordnance velocities, a large amount of plastic deformation of the target and penetrator occurs as the penetrator burrows through the target. The target material is generally displaced or pushed aside by the moving penetrator-target interface while the penetrator continually erodes away. The influence of the penetrator's material characteristics (density, mechanical properties, etc.) on its ballistic performance have been modeled analytically (Tate 1967; Frank and Zook 1986) and computationally, using 2- and 3-dimensional finite element hydrocodes (Zukas et al. 1981). Many aspects of the flow and failure process during penetration remain difficult to model and do not adequately reflect the differences in penetration seen experimentally between DU and WHA.

In Figure 6, the penetration depths into RHA, normalized by penetrator length, of a WHA (90W-7Ni-3Fe, 17.2 g/cm³) (Sorensen et al. 1989; Magness 1990a), the U-3/4Ti alloy (18.6 g/cm³) tested in this study, and a similar U-3/4Ti alloy tested by Magness (1990a) are compared as a function of impact velocity. All four sets of data represent penetrator cores which have an aspect ratio of 20. The two data sets in the ordnance velocity regime are quarter-scale penetrators, and the two data sets in the higher velocity portion of the plot (greater than 1.7 km/s) are approximately half-scale penetrators. Some small scaling effect due to large differences in penetrator diameters is expected to offset the quarter-scale data set slightly lower than the half-scale data set; however, they both were included on the same plot to show the overall trend of the data as velocity is increased to the high velocity regime.

At ordnance velocities less than 1.8 km/s, the DU alloy has an approximate 100 m/s performance edge over the 90% WHA. Some may argue that the DU alloy penetrates deeper because it has a higher density than the 90% WHA. However, Figure 7 shows that this is not the case. An equal density (18.6 g/cm³), 97% WHA penetrator is compared to a geometrically equivalent ($L/D = 10$) DU alloy penetrator (Farrand 1990). The performance gap between the two alloys still exists at ordnance velocities and, therefore, should not be attributed to simply a density advantage but rather attributed to some inherent deformation and flow properties not yet completely understood. There have been several different explanations offered for the superior penetration performance of the U3/4Ti alloy at ordnance velocities, and most find their roots in the fundamental differences in the metallurgy and mechanical properties of WHA and DU alloys. More recently, Magness (1990b) has proposed a penetration model which uses the phenomenon of adiabatic shear to explain the performance differences between the two alloys.

In Figures 6 and 7, as the impact velocities exceed the ordnance velocity regime, the penetration performance differences between DU and WHA diminish. The penetration convergence suggests that the deformation and flow properties of both alloys become similar at higher impact velocities. The velocity at which the two alloys appear to converge (1.9 km/s–2.0 km/s) approaches the velocity regime for which the so-called hydrodynamic penetration theory of rods applies. The classic solution of the penetration of a fluid jet into a semi-infinite target was first derived by Birkhoff et al., and it represents the depth of penetration of a shaped charge jet into a metallic target (Equation 2). For very high velocity penetration, this equation has been used to represent the depth of penetration of a long rod penetrator into a metallic target. The penetration event in this case is described as a hydrodynamic

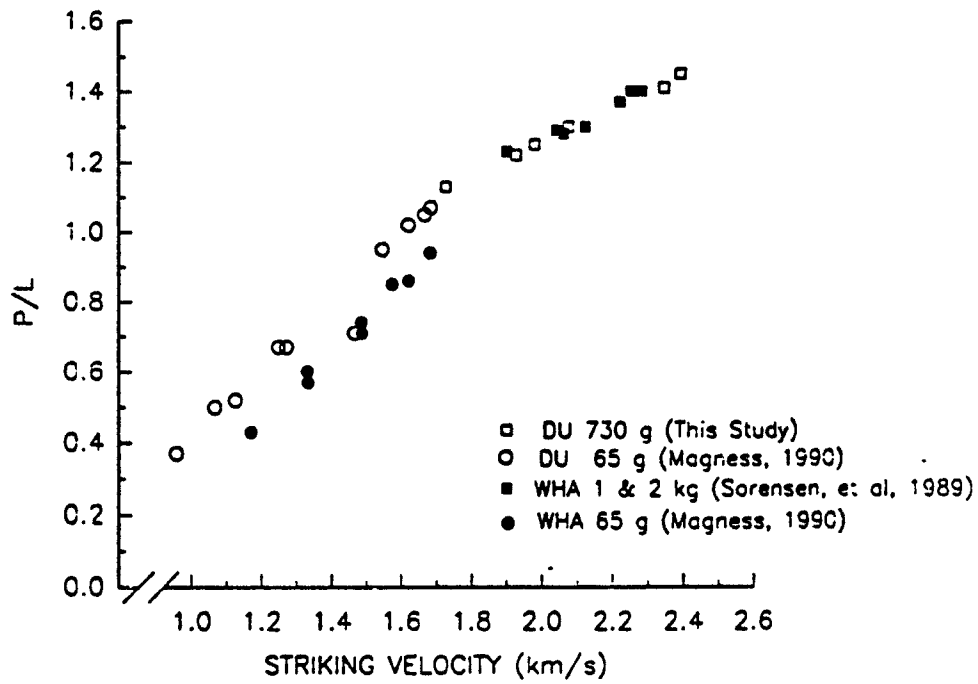


Figure 6. L/D=20 DU and 90% WHA Penetration Data Compared.

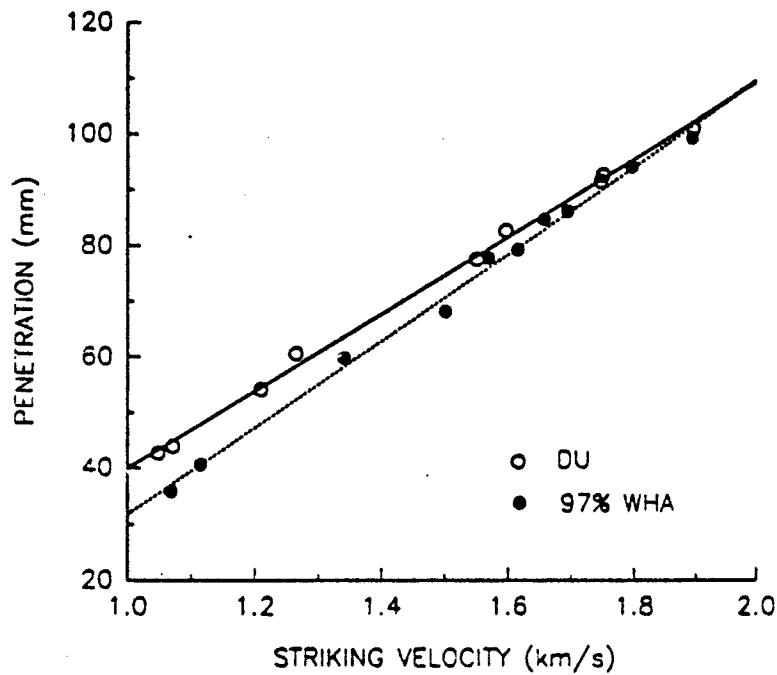


Figure 7. L/D=10 DU and 97% WHA Penetration Data Compared (Farrand 1990).

process in which there exists a theoretical upper limit of penetration. This upper limit is defined by the following equation:

$$P/L = \sqrt{\rho_p/\rho_T} \quad (2)$$

where P = depth of penetration
 L = penetrator length
 ρ_p = penetrator density
 ρ_T = target density.

The interesting aspect of this equation is that the depth of penetration is a function of the penetrator length and the penetrator and target densities but not the impact velocity. At high velocities, the impact pressures are so much greater than the penetrator and target material strengths that the strengths can be ignored. Although the theoretical hydrodynamic limit does not agree perfectly with experimental test results, previous penetration data of long rod WHA alloys into RHA show that depth of penetration approaches an asymptotic limit (see Figure 8) (Sorensen et al. 1989).

The comparative data sets of DU and WHA alloys in Figure 6 and 7 can be characterized as being in the transitional region between the ordnance velocity and the theoretical hydrodynamic limit. As the impact velocities are increased, a larger percentage of the penetration process is hydrodynamic in nature, and, therefore, theoretically more dependent only on penetrator and target densities. The difference between the densities of the DU alloy and 90%-W content WHA alloy is small enough so that the slight performance difference predicted by the hydrodynamic theory is indistinguishable amongst the standard deviation of the data points in Figure 6.

6. CONCLUSIONS

The objective of this program was to establish the penetration capabilities of depleted uranium at high velocity impacts so that 1) it may be compared to the high velocity penetration capabilities of its tungsten counterpart, and 2) it may be used as a baseline for evaluating the performance of advanced armor technologies against similar impact conditions.

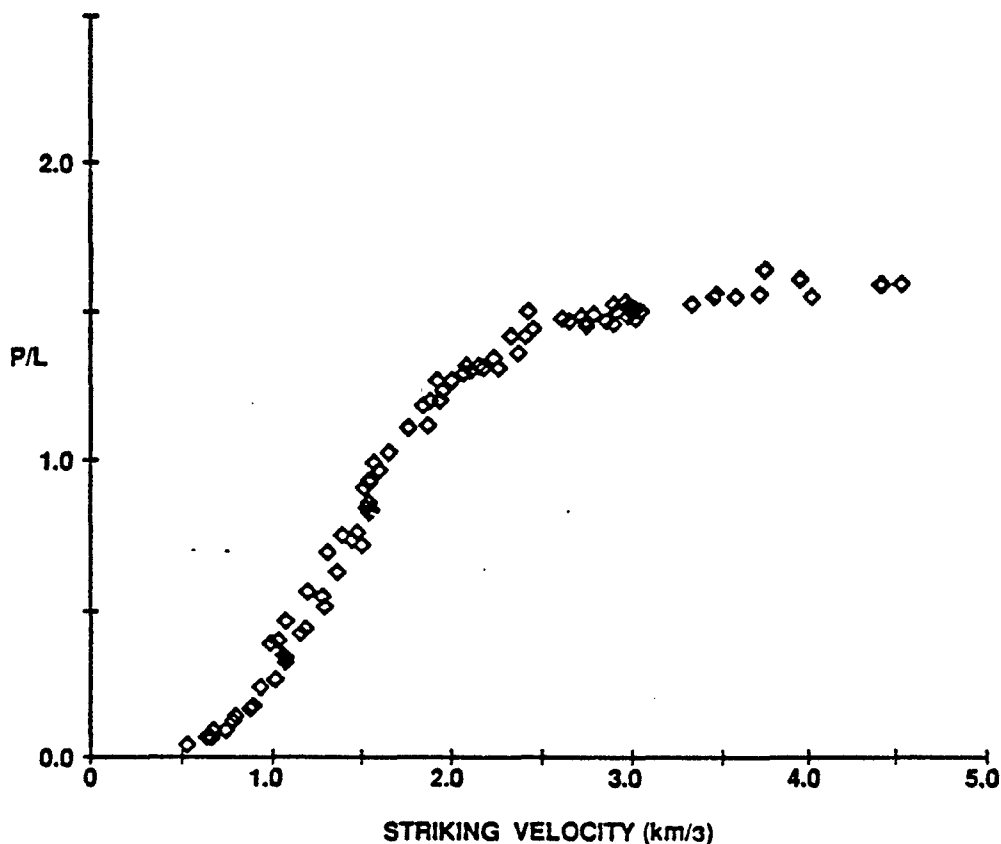


Figure 8. Semi-Infinite RHA Penetration by 90% WHA L/D 9-30 Penetrators (Sorensen et al. 1989).

The penetration performance of a half-scale, long rod, KE projectile with a depleted uranium alloy (U-3/4Ti) core has been established against semi-infinite RHA at impact velocities up to 2.4 km/s. A direct comparison of the penetration results from similar tests using a comparable aspect ratio, tungsten heavy alloy penetrator revealed that as the impact velocities approach the high velocity regime (greater than 2.0 km/s), the penetration performances of the two materials converge. At ordnance velocities, the inherent material properties of DU make it a superior penetrator. However, at higher impact velocities, the inertial effects characteristic of hydrodynamic penetration appear to dominate the penetration process resulting in nearly equal penetration performance of DU and WHA alloy long rod penetrators. Future high velocity testing efforts will focus on advanced armor technologies and comparisons with geometric equivalent tungsten alloy penetrator performance.

INTENTIONALLY LEFT BLANK.

7. REFERENCES

- Birkhoff, G., D. P. Macdougall, E. M. Pugh, and G. Taylor. "Explosives With Lined Cavities." Journal of Applied Physics, vol. 19, no. 6, pp. 563-582, 1948.
- Bjerke, T. W., G. F. Silsby, R. M. Mudd, and D. R. Scheffler. "Yawed Long-Rod Armor Penetration at Ordnance and Higher Velocities." BRL-TR-3221, U.S. Army Ballistic Research Laboratory, Aberdeen Proving Ground, MD, March 1991.
- Colburn, J., M. Keele, and J. Bowen. "High Velocity Slug Firings of Slug Projectiles in a Double Travel 120-mm Gun System." BRL-MR-3906, U.S. Army Ballistic Research Laboratory, Aberdeen Proving Ground, MD, April 1991.
- Drysdale, W. H. "Design of Kinetic Energy Projectiles for Structural Integrity." BRL-TR-02365, U.S. Army Ballistic Research Laboratory, Aberdeen Proving Ground, MD, September 1981.
- Farrand, T. Unpublished terminal ballistic data. U.S. Army Ballistic Research Laboratory, Aberdeen Proving Ground, MD, 1990.
- Frank, K., and J. Zook. "Energy-Efficient Penetration and Perforation of Targets in the Hypervelocity Regime," Proceedings of the 1986 Hypervelocity Impact Symposium, 1986.
- Hohler, V., and A. J. Stulp. "Penetration of Steel and High Density Rods in Semi-Infinite Steel Targets." Proceedings of the Third International Symposium on Ballistics, 23-25 March 1977.
- Kennedy, E. W., and R. S. Coates. "Terminal Ballistic Evaluation of .35 Scale Depleted Uranium and Tungsten Heavy Alloy Penetrators vs. RHA Targets." BRL-MR-3850, U.S. Army Ballistic Research Laboratory, Aberdeen Proving Ground, MD, July 1990a.
- Kennedy, E. W., and R. S. Coates. "Tungsten Heavy Alloy Kinetic Energy Penetrators vs. RHA Steel Targets." BRL-MR-3858, U.S. Army Ballistic Research Laboratory, Aberdeen Proving Ground, MD, August 1990b.
- Magness, L. "Evaluation of Depleted Uranium alloys for Use in the XM881, 25-mm APFSDS-T Cartridge." BRL-MR-3563, U.S. Army Ballistic Research Laboratory, Aberdeen Proving Ground, MD, December 1986.
- Magness, L. Unpublished terminal ballistic data. U.S. Army Ballistic Research Laboratory, Aberdeen Proving Ground, MD, 1990a.
- Magness, L. "Deformation Behavior and its Relationship to the Penetration Performance of High Density Kinetic Energy Penetrator Materials." Paper presented at the Army Science Conference, Raleigh, NC, June 1990b.
- Silsby, G. F. "Penetration of Semi-Infinite Steel Targets by Tungsten Long Rods at 1.3 to 4.5 km/s." Proceedings of the 8th International Symposium on Ballistics, October 1984.

Silsby, G. F., R. J. Roszak, and L. G. Giglio-Tos. "BRL's 50-mm High Pressure Powder Gun for Terminal Ballistic Testing—The First Year's Experience." BRL-MR-03236, U.S. Army Ballistic Research Laboratory, Aberdeen Proving Ground, MD, January 1983.

Sorensen, B., K. Kimsey, G. Silsby, D. Scheffler, T. Sherrick, and W. de Fosset. "High Velocity Penetration of Steel Targets." Presented at the 1989 High Velocity Impact Symposium, San Antonio, TX, 12-14 December 1989.

Tate, A. "A Theory for the Deceleration of Long Rods After Impact" Journal of Mechanical Physics and Solids, vol. 387, 1967.

Zukas, J. A., G. H. Jonas, K. D. Kimsey, J. J. Misey, and T. M. Sherrick. "Three Dimensional Impact Simulations: Resources and Results." Computer Analysis of Large-Scale Structures, AMD, vol. 49, American Society of Mechanical Engineering, 1981.

<u>No. of Copies</u>	<u>Organization</u>	<u>No. of Copies</u>	<u>Organization</u>
2	Administrator Defense Technical Info Center ATTN: DTIC-DDA Cameron Station Alexandria, VA 22304-6145	1	Commander U.S. Army Missile Command ATTN: AMSMI-RD-CS-R (DOC) Redstone Arsenal, AL 35898-5010
1	HQDA (SARD-TR) WASH DC 20310-0001	1	Commander U.S. Army Tank-Automotive Command ATTN: ASQNC-TAC-DIT (Technical Information Center) Warren, MI 48397-5000
1	Commander U.S. Army Materiel Command ATTN: AMCDRA-ST 5001 Eisenhower Avenue Alexandria, VA 22333-0001	1	Director U.S. Army TRADOC Analysis Command ATTN: ATRC-WSR White Sands Missile Range, NM 88002-5502
1	Commander U.S. Army Laboratory Command ATTN: AMSLC-DL 2800 Powder Mill Road Adelphi, MD 20783-1145	1	Commandant U.S. Army Field Artillery School ATTN: ATSF-CSI Ft. Sill, OK 73503-5000
2	Commander U.S. Army Armament Research, Development, and Engineering Center ATTN: SMCAR-IMI-1 Picatinny Arsenal, NJ 07806-5000	(Class. only) 1	Commandant U.S. Army Infantry School ATTN: ATSH-CD (Security Mgr.) Fort Benning, GA 31905-5660
2	Commander U.S. Army Armament Research, Development, and Engineering Center ATTN: SMCAR-TDC Picatinny Arsenal, NJ 07806-5000	(Unclass. only) 1	Commandant U.S. Army Infantry School ATTN: ATSH-CD-CSO-OR Fort Benning, GA 31905-5660
1	Director Benet Weapons Laboratory U.S. Army Armament Research, Development, and Engineering Center ATTN: SMCAR-CCB-TL Watervliet, NY 12189-4050	1	Air Force Armament Laboratory ATTN: WL/MNOI Eglin AFB, FL 32542-5000 <u>Aberdeen Proving Ground</u>
(Unclass. only) 1	Commander U.S. Army Armament, Munitions and Chemical Command ATTN: AMSMC-IMF-L Rock Island, IL 61299-5000	2	Dir, USAMSAA ATTN: AMXSY-D AMXSY-MP, H. Cohen
1	Director U.S. Army Aviation Research and Technology Activity ATTN: SAVRT-R (Library) M/S 219-3 Ames Research Center Moffett Field, CA 94035-1000	1	Cdr, USATECOM ATTN: AMSTE-TD
		3	Cdr, CRDEC, AMCCOM ATTN: SMCCR-RSP-A SMCCR-MU SMCCR-MSI
		1	Dir, VLAMO ATTN: AMSLC-VL-D
		10	Dir, BRL ATTN: SLCBR-DD-T

<u>No. of</u> <u>Copies</u>	<u>Organization</u>
1	Office of the Assistant Secretary for Research and Development and Acquisition U.S. Department of the Army (SARD) ATTN: Irena Szkrybalo The Pentagon, Room 3E474 Washington, DC 20310
1	Commander U.S. Army Missile Command ATTN: AMSMI-RD, George Snyder Redstone Arsenal, AL 35898-5010
1	Commander U.S. Army Tank-Automotive Command ATTN: SFAE-ASM-SS-T, T. Dean Warren, MI 48397-5000
2	Director Lawrence Livermore National Laboratory ATTN: Carl Cline Al Holt P.O. Box 908 Livermore, CA 94550
1	Director Los Alamos National Laboratory ATTN: Billy Hogan P.O. Box 1663 Los Alamos, NM 87545
1	Director Sandia National Laboratories ATTN: James Assay P.O. Box 5800 Albuquerque, NM 87185
1	Southwest Research Institute ATTN: C. Anderson 6220 Culebra Road P.O. Drawer 28510 San Antonio, TX 78284
1	California Research and Technology Corporation ATTN: Dennis Orphal 5117 Johnson Drive Pleasanton, CA 94566

<u>No. of</u> <u>Copies</u>	<u>Organization</u>
1	Kaman Sciences Corporation ATTN: D. Barnette P.O. Box 7463 Colorado Springs, CO 80933
1	General Research Corporation ATTN: Alex Charters 5303 Hollister Ave. Santa Barbara, CA 93160-6770
1	Dupont ATTN: Robert Brunner Chestnut Run - CR702 Wilmington, DE 19898
1	Battelle ATTN: Stan Goddard 505 King Ave. Columbus, OH 43201-2693
1	University of Dayton Research Institute ATTN: Dr. S.J. Bless P.O. Box 283 Dayton, OH 45409

**No. of
Copies Organization**

**1 Rafael, Ordnance and Systems Division
ATTN: Dr. Gideon Rosenberg
P.O. Box 2250
Haifa, Israel 31021**

INTENTIONALLY LEFT BLANK.

USER EVALUATION SHEET/CHANGE OF ADDRESS

This laboratory undertakes a continuing effort to improve the quality of the reports it publishes. Your comments/answers below will aid us in our efforts.

1. Does this report satisfy a need? (Comment on purpose, related project, or other area of interest for which the report will be used.) _____

2. How, specifically, is the report being used? (Information source, design data, procedure, source of ideas, etc.) _____

3. Has the information in this report led to any quantitative savings as far as man-hours or dollars saved, operating costs avoided, or efficiencies achieved, etc? If so, please elaborate. _____

4. General Comments. What do you think should be changed to improve future reports? (Indicate changes to organization, technical content, format, etc.) _____

BRL Report Number BRL-TR-3236 Division Symbol _____

Check here if desire to be removed from distribution list. _____

Check here for address change. _____

Current address: Organization _____
Address _____

DEPARTMENT OF THE ARMY
Director
U.S. Army Ballistic Research Laboratory
ATTN: SLCBR-DD-T
Aberdeen Proving Ground, MD 21005-5066



NO POSTAGE
NECESSARY
IF MAILED
IN THE
UNITED STATES

OFFICIAL BUSINESS

BUSINESS REPLY MAIL
FIRST CLASS PERMIT No 0001, AFG, MD

Postage will be paid by addressee

Director
U.S. Army Ballistic Research Laboratory
ATTN: SLCBR-DD-T
Aberdeen Proving Ground, MD 21005-5066

